

On inhomogeneous nonholonomic Bilimovich system

A.V. Borisov⁽¹⁾, E.A. Mikishanina⁽²⁾, A.V. Tsiganov⁽¹⁾

⁽¹⁾ Steklov Mathematical Institute of Russian Academy of Sciences, Moscow, Russia

⁽²⁾ Chuvash State University, Cheboksary, Russia

borisov@rccd.ru, evaeva_84@mail.ru, andrey.tsiganov@gmail.com

Abstract

We consider a simple motivating example of non-Hamiltonian dynamical system with time-dependent constraint obtained by imposing rheonomic nonintegrable Bilimovich's constraint on a freely rotating rigid body. Dynamics of this low-dimensional nonlinear nonautonomous dynamic system involves different kinds of stable and unstable attractors, quasi and strange attractors, compact and noncompact invariant attractive curves, etc. We apply the Poincaré map method to study this cautionary example in order to disambiguate and discover multiscale temporal dynamics, specifically the coarse-grained dynamics which results from fast-scale nonlinear control via nonholonomic Bilimovich's constraint.

1 Introduction

Consider motion of a rigid body under its own inertia subjected to the rheonomic constraint

$$f = p - g(t)q - \alpha = 0 \quad (1.1)$$

where $\omega = (p, q, r)$ is an angular velocity vector in the body frame, $f(t)$ is an arbitrary function and a is an arbitrary constant. A system with homogeneous constraint (1.1) was studied by Bilimovich [2] at $\alpha = 0$ as a rheonomic generalization of the scleronomic Suslov system [14, 12]. In [2] Bilimovich also suggested a physical realization of this time-dependent constraint.

According to [2] at $\alpha = 0$ constraint (1.1) is the so-called ideal or perfect constraint, and we have a dynamical system in three-dimensional phase space with one constraint (1.1) and one integral of motion

$$T = \frac{1}{2}(\mathbb{I}\omega, \omega), \quad (1.2)$$

where \mathbb{I} is the inertia tensor of the body. Thus, at $\alpha = 0$ we have an integrable by quadratures system, see [2, 9] and references within.

In this note we suppose that $\alpha \neq 0$ and $g(t)$ is a periodic function which allows to study the inhomogeneous Bilimovich system by using the Poincaré map, which is an integral aspect of our understanding and analysis of nonlinear dynamical systems.

In [15] Henri Poincaré laid the foundations of what would become modern dynamical systems. In particular, he proposed to study the three-body problem by using the first recurrence map, or Poincaré map, characterizing intersection of a periodic orbit in the state space of a continuous dynamical system with a lower-dimensional subspace transverse to the flow. Nowadays, the principal method for identifying dynamic behavior of a nonlinear system includes the Lyapunov index method, Poincaré map method, bifurcation theory, etc [13, 16]. In practice it is difficult to explicitly calculate Poincaré maps for these given dynamical system because there are no general methods for their construction, but the advent of data-driven modeling techniques provides a set of regression techniques, broadly falling under the aegis of machine learning, which can discover and/or fit dynamical models to the time series measurements of a dynamical system [1, 10, 11].

Dynamics on the Poincaré map preserves many of the periodic and quasi-periodic orbits of the original system, and due to its dimensionally reduced form, it is often simpler to analyze than the

original system. This was especially true for celestial mechanics which was ideally suited for analysis via Poincaré maps [15] because Poincaré maps provide for a time scale separation by producing snapshots of dynamics on a sampling scale of the map period. In this note we show that it can be also true for nonholonomic systems with periodic rheonomic constraints. The Bilimovich system is chosen as a sample toy-model.

2 Bilimovich system with periodic rheonomic constraint

Let us take Euler equations of motion

$$\mathbb{I}\dot{\omega} = \mathbb{I}\omega \times \omega \quad \omega = (p, q, r).$$

where \times denotes a vector product in \mathbb{R}^3 , and assume that the body frame is oriented in such way that constraint $f = 0$ has fixed form (1.1). In this frame inertia tensor \mathbb{I} is a symmetric positive definite 3×3 matrix.

Equations of motion for the constrained system are obtained via the Lagrange D'Alembert principle that yields

$$\mathbb{I}\dot{\omega} = \mathbb{I}\omega \times \omega + \lambda \frac{\partial f}{\partial \omega}, \quad \frac{\partial f}{\partial \omega} = \begin{pmatrix} 1 \\ -g(t) \\ 0 \end{pmatrix} \quad (2.3)$$

where Lagrange multiplier λ is determined on condition that the constraint is satisfied

$$\frac{df}{dt} = \left(\frac{\partial f}{\partial \omega}, \dot{\omega} \right) + \frac{\partial f}{\partial t} = 0,$$

Here (x, y) denotes the scalar product of two vectors in \mathbb{R}^3 . Using the equation of motion we obtain

$$\lambda = - \frac{\left(\frac{\partial f}{\partial \omega}, \mathbb{I}^{-1}(\mathbb{I}\omega \times \omega) \right) + \frac{\partial f}{\partial t}}{\left(\mathbb{I}^{-1} \frac{\partial f}{\partial \omega}, \frac{\partial f}{\partial \omega} \right)}.$$

Equations of motion (2.3) with this λ preserve the quantity $p - g(t)q$. On the level set $p - g(t)q = \alpha$ we can substitute $p = \alpha + g(t)r$ into (2.3) and obtain a nonautonomous system of equations in the (q, r) plane

$$\dot{q} = Q(q, r, t) \quad \text{and} \quad \dot{r} = R(q, r, t). \quad (2.4)$$

Any periodically forced nonautonomous differential equation can be represented in terms of an autonomous flow in a torus. To achieve this transformation, simply introduce the third variable $s(t) = t$. The two dimensional system of equations (2.4) then becomes a three dimensional autonomous system defined by equations

$$\dot{q} = Q(q, r, s), \quad \dot{r} = R(q, r, s), \quad \dot{s} = 1. \quad (2.5)$$

The flow in this state space corresponds to the trajectory of flowing around a torus with period 2π . This naturally leads to a Poincaré section at $s = t_0$. The Poincaré map method is a standard tool to determine stability, chaos and bifurcations for a periodically forced nonautonomous system of differential equations [13, 16].

So, we take periodic functions $g(t) = g(t + T)$ and numerically solve the system of equations (2.4) with random initial conditions $q(t_0) = q_0$ and $r(t_0) = r_0$. As a result, we obtain a set of points x_k on (q, r) -plane with coordinates

$$q_k = q(t_0 + kT) \quad \text{and} \quad r_k = r(t_0 + kT), \quad k = 0, \dots, N.$$

The Poincaré map is a discrete map

$$\begin{pmatrix} q_k \\ p_k \end{pmatrix} \rightarrow \begin{pmatrix} q_{k+1} \\ p_{k+1} \end{pmatrix}, \quad \text{or} \quad x_{k+1} = F(x_k). \quad (2.6)$$

Study of autonomous systems usually begins with solving of equations

$$Q(q, r, s) = 0, \quad R(q, r, s) = 0, \quad (2.7)$$

with respect to q and r in order to get equilibrium points (q_i^*, p_i^*) on the (q, r) -plane. In our case equations (2.7) may have two, three or four solutions depending on the parameter values. Existence of a different number of solutions allows us to explore the various Poincaré maps with different kinds of equilibrium points, attractors and strange attractors, compact and noncompact attractive curves, etc.

2.1 Two critical points

If \mathbb{I} is a diagonal inertia tensor

$$\mathbb{I}_{12} = \mathbb{I}_{13} = \mathbb{I}_{23} = 0,$$

then equations (2.4) are equal to

$$\begin{aligned} \frac{dq(t)}{dt} &= Q(q, r, t) \equiv -\frac{1}{g(t)^2 \mathbb{I}_{11} + \mathbb{I}_{22}} \left(\alpha (\mathbb{I}_{11} - \mathbb{I}_{33}) r(t) + g(t) (\mathbb{I}_{11} - \mathbb{I}_{22}) q(t) r(t) + g(t) \frac{dg(t)}{dt} \mathbb{I}_{11} q(t) \right), \\ \frac{dr(t)}{dt} &= R(q, r, t) \equiv \frac{(\mathbb{I}_{11} - \mathbb{I}_{22}) (g(t) q(t) + \alpha) q(t)}{\mathbb{I}_{33}}. \end{aligned}$$

If $g(t) = g(-t)$, the equations are invariant with respect to involution

$$t \rightarrow -t, \quad q \rightarrow q, \quad r \rightarrow -r.$$

So, trajectories in the manifold of states of motion are grouped in symmetric pairs and, therefore, on the Poincaré maps the attractors and repellers meet in pairs which are symmetrical with respect to the replacement.

The two solutions of the corresponding system of equations (2.7) have the following form

$$x_1^* = (0, 0) \quad \text{and} \quad x_2^* = \left(-\frac{\alpha}{g(t)}, \frac{\mathbb{I}_{11}}{(\mathbb{I}_{22} - \mathbb{I}_{33})} \frac{dg(t)}{dt} \right). \quad (2.8)$$

These solutions are the counterparts of equilibrium points for the Poincaré maps for the periodically forced nonautonomous system (2.4).

Below we put $g(t) = \cos t$ and $t_0 = 0$, so that

$$x_1^* = (0, 0), \quad \text{and} \quad x_2^* = \left(-\frac{\alpha}{\cos t}, \frac{\mathbb{I}_{11}}{(\mathbb{I}_{22} - \mathbb{I}_{33})} \sin(t) \right), \quad (2.9)$$

and present the Poincaré section data obtained by numerical integration of (2.4).

In generic cases at

$$\mathbb{I}_{11} < \mathbb{I}_{22} < \mathbb{I}_{33} \quad \text{and} \quad \mathbb{I}_{11} > \mathbb{I}_{22} > \mathbb{I}_{33}$$

The Poincaré sections possess noncompact attractive curves in contrast with other cases when all the trajectories are compact. Let us present a few Poincaré sections for equations (2.4) with noncompact attractive curves at

$$A : \mathbb{I} = \text{diag}(1, 2, 4), \quad B : \mathbb{I} = \text{diag}(4, 2, 1)$$

and with compact attractive curves at

$$C : \mathbb{I} = \text{diag}(1, 4, 2), \quad D : \mathbb{I} = \text{diag}(4, 1, 2).$$

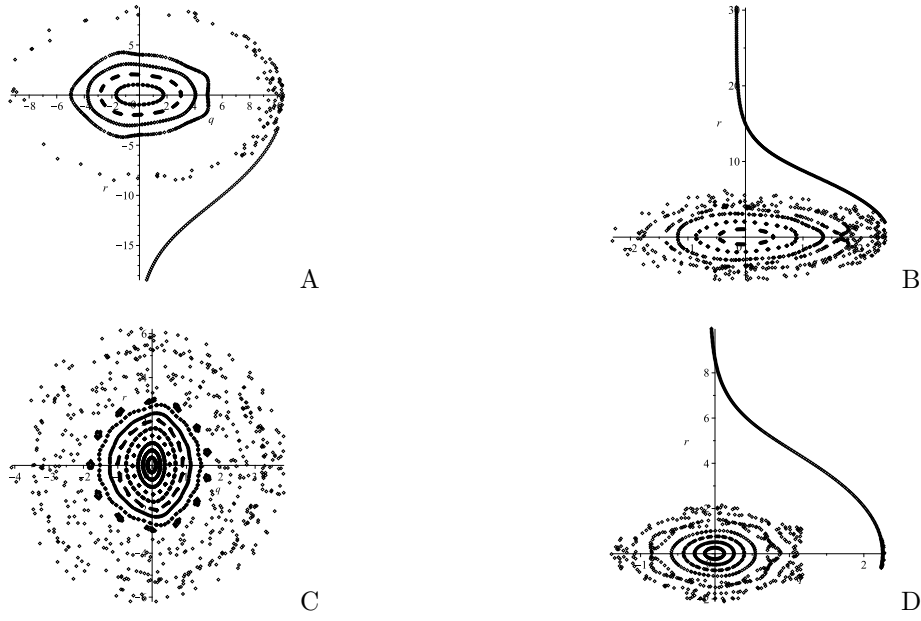


Figure 1: Poincaré maps with compact and noncompact attractive curves at $\alpha = 0.1$

The Poincaré sections in Fig.1 A-B consist of invariant curves associated with the quasiperiodic solutions of (2.4), i.e. the so-called islands of critical tori, and chaotic trajectories turning into a noncompact attractive curve. In Fig.1 C-D we can also find invariant curves associated with the quasiperiodic solutions of (2.4) and an attractive invariant curve corresponding to a crescent moon-shaped torus in phase space.

The crescent moon-shaped curves have merged to form a single island of tori in phase space at $\alpha = 0.4$ which is shown in Fig.2



Figure 2: Poincaré maps with crescent moon-shaped curves at $\alpha = 0.4$

The many points existing outside these two islands are situated in a region through which pass the unstable aperiodic orbits in this section $t_0 = 0$.

If the time derivative of kinetic energy

$$\delta T = \frac{dT}{dt} = \alpha \lambda = -\alpha \frac{\left(\frac{\partial f}{\partial \omega}, \mathbb{I}^{-1}(\mathbb{I} \omega \times \omega) \right) + \frac{\partial f}{\partial t}}{\left(\mathbb{I}^{-1} \frac{\partial f}{\partial \omega}, \frac{\partial f}{\partial \omega} \right)}$$

in the given region of phase space is always greater than zero, then rotation of the rigid body accelerates. If δT is always less than zero, then the rotation attenuates. If δT is alternating, then trajectories of the rigid body in velocity space will be compact.

Exact estimation of derivative δT in the given region of phase space is a rather cumbersome task, which can be solvable using the Poincaré map method. For instance, let us consider data from

ten random trajectories turning into a noncompact attractive curve in Fig.1A. Results of numerical integration of (2.4) with initial conditions $q_0 = 0$ and $r_0 = 8$ are presented in Fig.3.



Figure 3: Poincaré section data q_k and r_k at $\alpha = 0.1$

At the interval of $k = 200 \dots 900$ we can fit a univariate polynomial to data q_k and r_k by minimizing the least-squares error. Averaging coefficients of ten such polynomials associated with random initial conditions we obtain

$$q(t) = -0.300263, \quad r(t) = -0.0002545t^2 - 0.2386278t + 26.779718 = at^2 + bt + c.$$

Thus, the Poincaré map in this region reads as

$$q_{k+1} = q_k, \quad r_{k+1} = r_k + 2\pi\sqrt{b^2 - 4ac + 4ar_k} + 4a\pi^2.$$

Although this mapping is not an exact representation of (2.6), it allows us to describe qualitative dynamics of the rigid body under Bilimovich's constraint (1.1). Indeed, we can say that in this region of phase space the first and second components of angular velocity are constants on average, whereas the absolute value of the third component increases.

At $\mathbb{I}_{13} = \mathbb{I}_{23} = 0$ equations (2.4) also have only two solutions. According to [9] in this case we can integrate the nonautonomous equations (2.4) in terms of hyperbolic functions at $\alpha = 0$.

2.2 Three critical points

At $\mathbb{I}_{12} = \mathbb{I}_{23} = 0$, equations (2.7) have two fixed solutions

$$x_1^* = \left(0, \frac{\mathbb{I}_{33} - \mathbb{I}_{11} \pm \sqrt{(\mathbb{I}_{11} - \mathbb{I}_{33})^2 + 4\mathbb{I}_{13}^2}}{2\mathbb{I}_{13}} \alpha \right)$$

and one solution depending on time. If

$$\mathbb{I} = \begin{pmatrix} 1 & 0 & 0.1 \\ 0 & 2 & 0 \\ 0.1 & 0 & 4 \end{pmatrix}, \quad g(t) = \cos t,$$

the Poincaré transversal plane at $t_0 = 0$ looks like



Figure 4: Poincaré maps at $\alpha = \pm 0.1$

In Fig.4A-B we can see quasi attractors for the system of nonautonomous equations (2.5). These quasi attractors have the following Lyapunov exponents

$$\lambda_1 = 0.022, \quad ad\lambda_2 = -0.034, \quad \lambda_3 = 0, \quad \sum_{i=1}^3 \lambda_i = -0.012,$$

and Lyapunov dimension

$$D = 1 + \frac{\lambda_1}{|\lambda_2|} = 1.647.$$

The values of Lyapunov exponents λ_i and dimension D are independent of the sign of parameter α .

This quasi attractor disappears with increase of $|\alpha|$, and one gets the islands of invariant curves associated with the quasiperiodic solutions and noncompact attractive curve at $\alpha = \pm 0.4$, see Fig.5 and Fig.6.

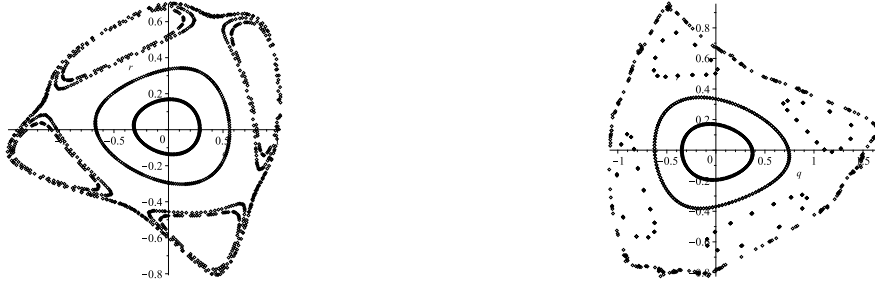


Figure 5: Central part of the Poincaré sections at $\alpha = \mp 0.4$



Figure 6: Poincaré sections with noncompact invariant curves at $\alpha = \mp 0.4$

At $\alpha = -0.4$, see Fig.6A, averaging by ten trajectories with random initial conditions, polynomials describing the Poincaré data at the interval of $k = 200 \dots 900$ are equal to

$$q(t) = -0.5241223 - 0.1461676 t, \quad r(t) = 0.00009 t^2 - 1.5651429 t + 7.4115722.$$

At $\alpha = 0.4$ these polynomials have the following form

$$q(t) = -2.7790128 - 0.14597897 t, \quad r(t) = 0.00009 t^2 - 1.5598174 t + 7.966923.$$

These quadratic polynomials $r(t)$ can only be used locally and bear little resemblance to the true map (2.6) at $k \rightarrow \infty$ because leading coefficients are positive.

In order to get an asymptotic we can fit this Poincaré section data by linear polynomials

$$\alpha = -0.4, \quad r(t) = -1.4616911 t - 17.1864607 \quad \text{and} \quad \alpha = 0.4 \quad r(t) = -1.459806 t - 15.8130501$$

or by cubic polynomials $r(t) = -at^3 + bt^2 + ct + d$ with negative leading coefficient $a \sim 5 \cdot 10^{-8}$. Another way is numerical integration of the equations of motion over a larger interval $[0, 2\pi k]$, $k > 900$ without precision loss.

In both cases we can say that absolute values of the angular velocity components increase in proportion to each other.

2.3 Four critical points

At $\mathbb{I}_{13} \neq 0$ and $\mathbb{I}_{23} \neq 00$, equations (2.7) have four solutions. Let us present a gallery of the Poincaré sections for the following inertia tensor

$$\mathbb{I} = \begin{pmatrix} 1 & 0 & 0.5 \\ 0 & 2 & 0.3 \\ 0.5 & 0.3 & 4 \end{pmatrix},$$

which is designed to illustrate the origin and destruction of a strange attractor.

In the first stage, periodic trajectories become quasiperiodic trajectories attracting to invariant curve in Fig.7A, which later forms an unstable focus in Fig.7B. Another part of the periodic trajectories form a stable focus and trajectories from an unstable focus or repeller which are attracted to a stable focus or attractor in Fig.7C.

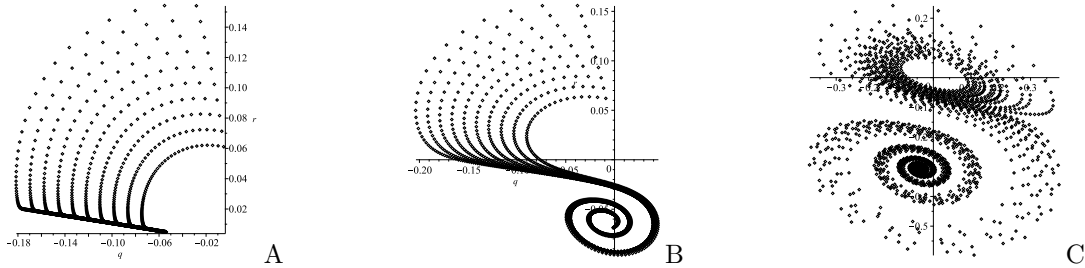


Figure 7: Poincaré sections at $\alpha = -0.001$, $\alpha = -0.01$ and $\alpha = -0.05$

In the second stage, the unstable focus goes into the strange attractor in Fig.8A-B and then the strange attractor disappears in Fig.8C. At the interval of $\alpha = -0.5.. -0.37$ rotation near a stable focus of few times changes directions from clockwise to counterclockwise and vice versa.

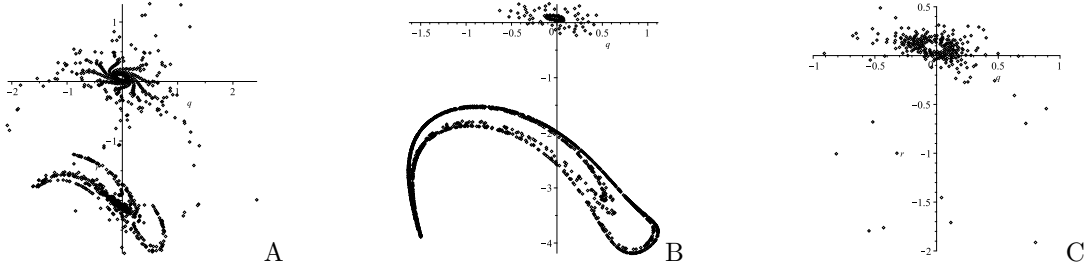


Figure 8: Poincaré sections at $\alpha = -0.37$, $\alpha = -0.45$ and $\alpha = -0.5$

For the strange attractor in Fig.8B the Lyapunov exponents are

$$\lambda_1 \simeq 0.082, \quad \lambda_2 \simeq -0.385, \quad \lambda_3 \simeq 0,$$

so its Lyapunov dimension is

$$D = 1 + \frac{\lambda_1}{|\lambda_2|} = 1.21.$$

It is compatible with a fractal dimension of the strange attractor for Hénon map $D = 1.26$ or Lorentz map $D = 2.07$.

As above, we can study the noncompact attractive curve given in Fig.9 at $\alpha = -0.45$.

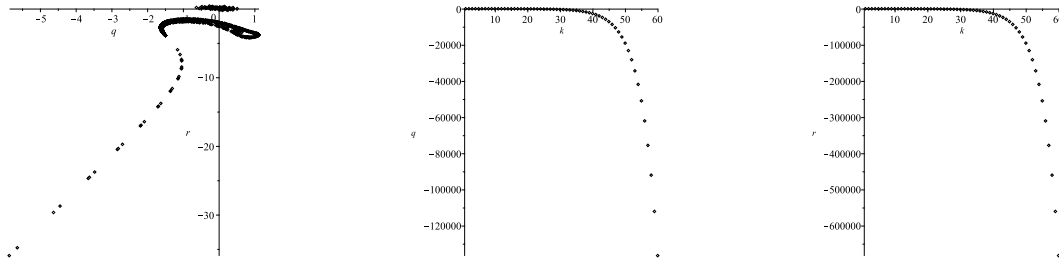


Figure 9: Poincaré section data and graphics of q_k and r_k at $\alpha = -0.45$

At the interval of $k = 0 \dots 60$ the best fitting is given by six order polynomials

$$q(t) = -0.0001t^6 + 0.0146t^5 + \dots, \quad r(t) = -0.0005t^6 + 0.073t^5 + \dots.$$

This polynomial fitting is most likely not optimal in the four critical points case, when a strange attractor is present in the Poincaré section.

3 Conclusion

Mathematically, the motion of the Euler top is described by geodesics of the left invariant metric on rotation group $SO(3)$. Physically, the Euler top is a rigid body moving about its center of mass without any forces acting on the body. It is one of the most studied systems in classical and quantum mechanics.

In [2] Bilimovich imposed a linear rheonomic constraint on the freely rotating rigid body, which preserves total mechanical energy, and as a result obtained an integrable time-dependent non-Hamiltonian system. Mechanical realization of this constraint proposed by Bilimovich is complex and most likely incorrect. Nevertheless, we suppose that classical effects such as free precession of a symmetric top, Feynmans wobbling plate, tennis-racket instability and the Dzhani­bekov effect, attitude control of satellites by momentum wheels, or twisting somersault dynamics, have their counterparts in this non-Hamiltonian system.

In this note we discuss the nonlinear counterpart of Bilimovich's constraint, which does not preserve total mechanical energy and which can be interpreted as a rigid body control. The corresponding 3D non-Hamiltonian system with a time depending constraint is reduced to a periodically forced 2D nonautonomous system of differential equations, which allows us to apply all the well-known machinery to study dynamic behavior of this system. We restrict ourselves by computing only a few of Poincaré maps, portraits of quasi and strange attractors, Lyapunov exponents, Lyapunov dimension and acceleration estimates. These computations have highlighted how the Poincaré map can be used to disambiguate and discover multiscale temporal dynamics, specifically the coarse-grained dynamics which results from fast-scale nonlinear control.

Of course, there are many other questions which have to be studied. For instance, the potential avenue for future work could come from applying of the Poincaré maps method and time piecewise feedback control laws on Bilimovich's constraint to stabilization of the limit cycles, to avoidance of areas with chaotic motion (strange attractors), to achievement of areas with acceleration for this periodically forced, non-autonomous, non-Hamiltonian system similar to [3, 4, 5, 6, 7, 8].

In fact, we find new very instructive example of nonholonomic system similar to Duffing oscillator, Rössler system, RC circuit, driven Brusselator, etc. This model system is related with the freely rotating rigid body in Hamiltonian mechanics, nonholonomic mechanics and control theory simultaneously.

This work of A.V. Borisov and A.V. Tsiganov was supported by the Russian Science Foundation (project no. 19-71-30012) and performed at the Steklov Mathematical Institute of the Russian Academy of Sciences. The authors declare that they have no conflicts of interest.

References

- [1] Ariel G., Engquist B., Kim S., Lee Y., Tsai R., em A multiscale method for highly oscillatory dynamical systems using a Poincaré map type technique J. Scientific Comp., v.54 (2-3), pp.247-268, 2013.
- [2] Bilimovich A. D. *Sur les systèmes conservatifs, non holonomes avec des liaisons dépendantes du temps*, Comptes Rendus Acad. Sci. Paris, v.156, pp.12-18, 1913, available from <https://gallica.bnf.fr/ark:/12148/bpt6k3109m/f1218.image.langFR>
- [3] Bizyaev I. A., Borisov A. V., Kuznetsov S. P., *Chaplygin sleigh with periodically oscillating internal mass*, v.119, 60008, 2017.
- [4] Bizyaev I A, Borisov A V, Mamaev I S. *Exotic Dynamics of Nonholonomic Roller Racer with Periodic Control*, Regular and Chaotic Dynamics, v.23, pp. 983-994, 2018.
- [5] Bizyaev I. A., Borisov A. V., Kozlov V. V., Mamaev I. S., *Fermi-like acceleration and power-law energy growth in nonholonomic systems*, Nonlinearity, v.32, pp.3209-3233, 2019.
- [6] Bizyaev I. A., Borisov A. V., Kuznetsov S. P., *The Chaplygin sleigh with friction moving due to periodic oscillations of an internal mass*, Nonlinear Dynamics, v. 95, pp. 699-714, 2019.
- [7] Borisov A. V., Kuznetsov S. P., *Regular and Chaotic Motions of a Chaplygin Sleigh under Periodic Pulsed Torque Impacts*, Regular and Chaotic Dynamics, v.21, pp. 792-803, 2016.
- [8] Borisov A.V., Kuznetsov S.P., *Comparing Dynamics Initiated by an Attached Oscillating Particle for the Nonholonomic Model of a Chaplygin Sleigh and for a Model with Strong Transverse and Weak Longitudinal Viscous Friction Applied at a Fixed Point on the Body*, Regular and Chaotic Dynamics, v. 23, pp. 803-820, 2018.
- [9] Borisov A. V., Tsiganov A.V., *On rheonomic nonholonomic deformations of the Euler equations proposed by Bilimovich*, submitted to Theor. Appl. Mechanics, 2020.
- [10] Bramburger J.J., Kutz J. N., *Poincaré Maps for Multiscale Physics Discovery and Nonlinear Floquet Theory*, arXiv:1908.10958, 2019.
- [11] Brunton S. L., Kutz J. N., *Data-driven science and engineering: Machine learning, dynamical systems and control*, Cambridge University Press, Cambridge UK, 2019.
- [12] Garcia-Naranjo L.C., Maciejewski A.J., Marrero J.C., Przybylska M., *The inhomogeneous Suslov problem*, Phys. Lett. A, v.378, pp. 2389-2394, 2014.
- [13] Kuznetsov, Yu. A., *Elements of Applied Bifurcation Theory*,: Springer, 3rd edition, 632 pages, 2004.
- [14] J. Neimark, N. Fufaev, *Dynamics of Nonholonomic Systems*, Transactions of Mathematical Monographs, v. 33, AMS, Providence, RJ, 1972.
- [15] Poincaré H., *Les methodes nouvelles de la mécanique céleste*, Gauthier-Villars, Paris, 1899.
- [16] Shilnikov L. P., *Method of Qualitative Theory in Nonlinear Dynmics*, Part 1-2, Higher Education Press, Beijing, China, 2010.